HHS Public Access

Author manuscript

Biochem Biophys Res Commun. Author manuscript; available in PMC 2021 September 03.

Published in final edited form as:

Biochem Biophys Res Commun. 2020 September 03; 529(4): 1106–1111. doi:10.1016/j.bbrc.2020.06.155.

Cathepsin K Is a Potent Disaggregase of α-Synuclein Fibrils

Ryan P. McGlinchey, **Shannon M. Lacy**, **Robert L. Walker III**, **Jennifer C. Lee***

Laboratory of Protein Conformation and Dynamics, Biochemistry and Biophysics Center, National Heart, Lung, and Blood Institute, National Institutes of Health

Abstract

The intracellular accumulation of α-synuclein (α-syn) amyloid fibrils is a hallmark of Parkinson's disease. Because lysosomes are responsible for degrading aggregated species, enhancing lysosomal function could alleviate the overburden of α-syn. Previously, we showed that cysteine cathepsins (Cts) is the main class of lysosomal proteases that degrade α-syn, and in particular, CtsL was found to be capable of digesting α-syn fibrils. Here, we report that CtsK is a more potent protease for degrading α-syn amyloids. Using peptide mapping by liquid chromatography with mass spectrometry, critical cleavage sites involved in destabilizing fibril structure are identified. CtsK is only able to devour the internal regions after the removal of both N- and C-termini, indicating their protective role of the amyloid core from proteolytic attack. Our results suggest that if overexpressed in lysosomes, CtsK has the potential to ameliorate α-syn pathology.

Graphical Abstract

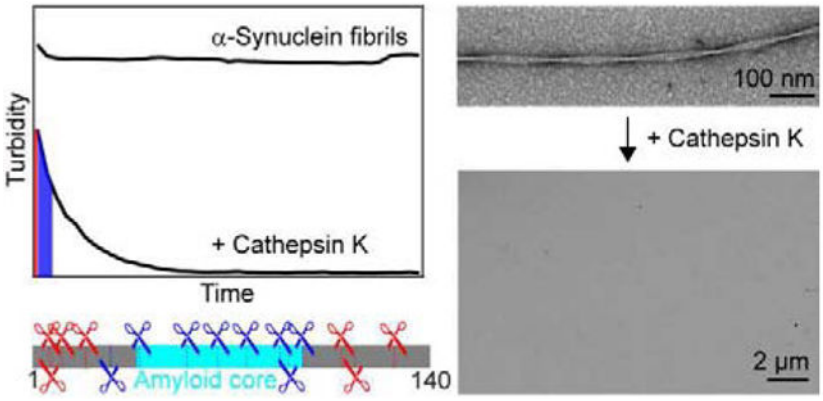

***Corresponding Author** leej4@nhlbi.nih.gov.

Author contributions

RPM and JCL designed the experiments. RPM, SML and RLW performed experiments. RPM and JCL wrote the manuscript. All the authors read and approved the manuscript.

Declaration of competing interest

The authors declare that they have no conflict of interest.

Declaration of competing interests

The authors declare that they have no known competing financial interests or personal relationships that could have appeared to influence the work reported in this paper.

Keywords

Parkinson’s disease; α-synuclein; cysteine cathepsin; LC-MS

1. Introduction

A pathological feature of Parkinson’s disease (PD) is the presence of Lewy bodies (LBs), intracytoplasmic inclusions rich in the protein α-synuclein (α-syn) [1]. The deposition of insoluble β-sheet-rich α-syn, generally referred to as amyloid, is a hallmark of the disease [2]. Various post-translational modifications and processing of α-syn, including phosphorylation and truncations are also associated with PD [3]. In the case of truncations, removal of the C-terminus accelerates the rate of aggregation both *in vitro* and *in vivo* [4-10].

An emerging cause for the build-up of α-syn and its C-terminal truncations is related to incomplete lysosomal degradation [11, 12]. Using lysosomes purified from brains of transgenic mice overexpressing the PD-associated A53T mutant (*SNCA*^{A53T}), increased levels of undigested α-syn and enrichment of C-terminal truncations were observed [12]. Despite the protein accumulation, there was no measurable loss of lysosomal proteolytic function, indicating that an overburden of aggregated α-syn is overwhelming the lysosome. Interestingly, > 60 % of the known α-syn truncations previously identified in LBs can be attributed to lysosomal protease activity.

α-Syn enters the lysosome through macroautophagy [13] or chaperone-mediated autophagy [14]. The main class of lysosomal proteases is the cathepsins (Cts) which are classified based on the active-site amino acids that confer catalytic activity, which are optimal in acidic pH (4.6–5) and most are inactive at neutral pH. These are cysteine (CtsB, CtsC, CtsF, CtsH, CtsK, CtsL, CtsO, CtsS, CtsV, CtsW, CtsX and asparagine endopeptidase), serine (CtsA and CtsG), and aspartyl (CtsD and CtsE) proteases [15-17]. CtsC, CtsX, and CtsA are exclusively exopeptidases, and all other proteases have endopeptidase activity. CtsB and CtsH has both endo- and exopeptidase activity.

In prior work, we showed that both CtsB and CtsL were primarily responsible for complete degradation of soluble α-syn, while CtsL was discovered to degrade α-syn amyloid fibrils [18]. CtsL acted on α-syn fibrils by first removing the C-terminus, followed by proteolysis of the β-sheet-rich core, composed of residues 30 to 100 [19]. Because many of these cleavages are at glycine residues, we suggested that β-turns are more vulnerable to proteolysis. However, there is limited endogenous CtsL activity *in vivo* [12] and considering the high levels of CtsL that was needed to degrade fibrils *in vitro*, we are motivated to search for an alternative, potent lysosomal protease towards the clearance of α-syn.

2. Materials and Methods

2.1. Protein and reagents

Recombinant α-synuclein was expressed in BL21(DE3) using human α-syn gene in a pRK172 plasmid [20]. For acetylated α-syn, the yeast NatB genes [21] were co-expressed

with α-syn gene. pRK172 plasmids for A30P, A53T, E46K, G51D and C-terminally truncated α-syn 1–122 were constructed using the Quick-change site-directed mutagenesis kit (Agilent), through the insertion of either a point mutation or a stop codon at the desired location. Proteins were purified as previously described [19]. Purity of α-syn was assessed by SDS-PAGE (NuPAGE 4-12% Bis-tris, Invitrogen) and confirmed by mass spectrometry (NHLBI Biochemistry Core). For acetylated α-syn, a minor population (~5%) of methionine-oxidized species are formed. Protein concentrations were determined using a molar extinction coefficient estimated on basis of amino-acid content: $\varepsilon_{280\ nm}$ = 5,960 M^{-1} cm^{-1}. Purified proteins were stored at −80 °C until use. All buffers were filtered (0.22 μm). Purified human liver cathepsins CtsB (C8571-25UG), CtsD (C8696-25UG), and CtsL (C6854-25UG), human leukocytes CtsG (C4428-0.25UN), human spleen CtsS (C5993-25UG), recombinant CtsF (SRP0290-50UG) and CtsV (SRP0293-10UG), Leupeptin (L2884.5MG), and ThT (T3516-5G) were purchased from Sigma Aldrich. Purified Cathepsin K (BML-SE553-0010) from insect cells was purchased from Enzo Life Sciences (Framingdale, NY). Recombinant CtsA (1049-SE) and CtsE (NP_001901) was purchased from R and D systems.

2.2. Fibril formation and degradation

Protein was exchanged into pH 5 (50 mM NaOAc, 20 mM NaCl) buffer using a PD-10 column (GE Healthcare) and filtered through YM-100 spin units (EMD Millipore) to remove any preformed aggregates prior to shaking in microcentrifuge tubes for several days at 37 °C in a VWR MiniMicro 980140 shaker (600 rpm). To prepare fibril samples at desired concentrations, they were pelleted at 16,100 × *g* for 10 min and resuspended in appropriate volume of buffer (50 mM NaOAc, 20 mM NaCl, 5 mM DTT, pH 5). Cts degradation (150 nM) was performed at 37 °C in microcentrifuge tubes using a MiniMicro 980140 shaker (300 rpm) and in clear, polystyrene, 384-well flat bottom microplates using a Tecan Infinite M200Pro microplate reader (1.0 mm orbital shaking) for SDS-PAGE analysis and turbidity (λ_{obs} = 400 nm) measurements, respectively.

2.3. Aggregation and seeding reactions

Aggregation was performed in sealed black, polypropylene, 384-well flat bottom microplates (781209, Greiner Bio-one). Seeds (1.5 μL from both 15 μM treated and untreated fibrils) were added to a α-syn solution ([α-syn] = 50 μM in 20 mM NaPi, 140 mM NaCl, pH 7.4). A CtsK inhibitor, leupeptin (1 μM) was added to all samples. Each well (40 μL) contained a 2-mm glass bead. ThT (5 μM) fluorescence (excited and monitored at 415 and 480 nm, respectively) was recorded as a function of time at 37 °C using a Tecan Spark microplate reader (1.0 mm linear shaking). A total of at least 2 independent experiments were performed with at least 5 replicates on each plate.

2.4. LC-MS analysis

In glass vials, soluble (15 μM) or fibrillar α-syn (15 or 30 μM) was incubated with CtsK (5–150 nM) in reaction buffer (50 mM NaOAc, 20 mM NaCl, 5 mM DTT, pH 5) in a total volume of 250 μL. Samples were agitated at 600 rpm at 37 °C in a Mini-Micro 980140 shaker. Reactions (40 μL) were taken at 15 min, 30 min, 1 h, 2 h, 4 h, 16 h and 20 h and terminated with 2M GuHCl. Samples (30 μL) were separated using a reverse-phase C18

column (Zorbax 300SB-C18, 2.1 x 50 mm, 3.5 μm, Agilent Technologies) on either a 1100 series HPLC (Agilent Technologies) coupled to an Agilent G1946D mass selective detector (MSD) equipped with an electrospray ionization (ESI) interface or Agilent 6224 accurate TOF-LC/MS (Agilent technology, Delaware). Mass spectra were obtained using positive-ion mode. Data were analyzed using LC/MSD ChemStation software (Rev. B.04.03, Agilent Technologies).

3. Results

3.1. Screening for a potent disaggregase of α-syn fibrils

To screen individual cathepsin activities, preformed α-syn fibrils (60 μM) were first incubated with CtsK, CtsB, CtsF, CtsL, CtsS, CtsV, CtsD, CtsE, CtsA, and CtsG (150 nM) and analyzed by SDS-PAGE (Fig. 1A and 1B). CtsF and CtsA had no effect and CtsB, CtsS, CtsV, CtsD, CtsE, and CtsG generated lower molecular weight fragments, corresponding to limited proteolysis. In contrast, CtsL and CtsK treatments of fibrils resulted in complete degradation. To discern which is more potent, we first carried out time course comparisons of CtsL and CtsK activities on soluble (Fig. 1C and 1D) and fibrillar α-syn (Fig. 1E and 1F). In both cases, CtsK was superior. Next, a turbidity assay was performed to monitor the reduction of scattered light as the insoluble materials are degraded. For a negative control, CtsB was used because it is unable to fully degrade fibrils. Consistent with SDS-PAGE, a more rapid loss in turbidity was observed with CtsK compared to CtsL, indicative of faster activity for CtsK (Fig. 1G).

To verify the loss of fibril structure, the amyloid sensitive dye, Thioflavin T (ThT) was added. For both CtsK and CtsL, there were negligible responses indicating the disappearance of amyloids compared to the untreated and CtsB-treated fibrils, which still exhibited high ThT enhancement (Fig. 1H). In support of this observation, liquid chromatography-mass-spectrometry (LC-MS) analysis taken after 20 h revealed the majority of the remaining peptide fragments to be < 2 kD (Fig. 1J, Table S1). No full-length protein was observed from CtsK treatment, while a small amount remained with CtsL. Clearly, our data show that CtsK is a stronger disaggregase.

Because some small peptides of α-syn have been shown to form self-complementary β-sheets, termed steric zippers, such as $_{47}$GVVHGVTTVA$_{56}$ and $_{68}$GAVVTGVTAVA$_{78}$ [22], we tested to see if any remaining peptides can serve as seeds in propagating amyloid formation. In the absence of seeds, α-syn proceeded with a lag phase followed by a elongation phase as monitored by ThT fluorescence. Addition of α-syn fibril seeds significantly hasten the aggregation kinetics. By comparison, in the presence of peptides from CtsK-treated fibrils, aggregation kinetics behaved similarly to the unseeded sample, suggesting negligible fibrillar remnants (Fig. 1K).

3.2. Peptide mapping CtsK degradation of soluble α-syn

To recapitulate its native form *in vivo*, N-terminally acetylated (Ac) α-syn was used for detailed peptide mapping analysis [23]. First, soluble Ac-α-syn (15 μM) was incubated with CtsK (5 nM), and aliquots were taken at different time points and analyzed by LC-MS (Fig.

2A). Peptides generated at the earliest time (15 min) were 1–9, 10–140, 1–27, 28–140, 1–53, 10–53, 54–140, 68–140, 1–75, 76–140, 1–114, and 115–140 (Fig. 2B, Table S2). Cleavage sites (denoted by X/X, where the slash indicates the cut) that generate these peptides are located throughout the α-syn sequence (Fig. 2C, red). In particular, A53/T54, G67/G68, and T75/A76 are located within the amyloidogenic region of α-syn. Continued incubation up to 2 h revealed additional peptide fragments generated from cuts within the amyloid core (Tables S2 and S3). These include cut positions at K6/G7, A17/A18, G25/V26, K34/E35, L38/Y39, G41/S42, G47/V48, A56/E57, T64/N65, A86/G87, A89/A90, and K96/K97 (Fig. 2C). After 16 h, most peptide masses were < 2 kD with additional cleavage sites (Table S4).

3.3. Peptide mapping CtsK degradation of α-synuclein fibrils

To monitor fibril degradation on a comparable time scale to soluble α-syn, a four-fold increase in CtsK was used. Preformed fibrils (15 μM) formed at pH 5 were incubated with CtsK (20 nM) and monitored as a function of time (Fig. 3A, Tables S5-S7). Samples for LC-MS analysis were prepared in an identical manner as described above. From the beginning, it is clear that degradation pattern of the fibrils was distinct with the appearance of N- and C-terminally truncated fragments, 10–140, 10–129, 10–114, and 10–109 (Fig. 3B, red, Table S5). These peptides resulted from cleavage sites at S9/K10, Q109/E110, E114/D115, and S129/E130 with the central portion untouched (Fig. 3C). By comparison, soluble α-syn is proteolyzed at A53/T54, G67/G68, and T75/A76 with two overlapping cleavage sites S9/K10 and E114/D115 that occurred in the N- (defined here as residues 1–35) and C-terminus (defined here as 97–140) at the earliest time.

After longer incubation, additional N-terminal cuts of the fibrils appeared first at A17/A18 (Fig. 3B, green, Table S5) and then at A27/E28 along with smaller peptides (Fig. 3B, magenta, Table S6), including many derived from within the amyloid-forming region such as 54–67, 68–75, and 76–89. These peptides increased with continued incubation with additional new peptides: 28–41, 39–45, 42–53, 54–64, 57–62, 57–75, and 76–86 (Fig. 3B, blue, Table S6). Interestingly, only after the appearance of fragment 28–109 do these smaller peptides begin to emerge, which also correspond to some of the initial cut sites observed for soluble α-syn at A53/T54, G67/G68, and T75/A76, in addition to positions L38/Y39, A89/A90, A91/T92, and K96/K97.

3.4. CtsK degradation of PD-related AcA53T mutant and C-terminal truncation Ac1–122

Next, we asked whether CtsK is efficient against two disease-related α-syn variants, A53T and C-terminally truncated Ac1–122. A53T has greater aggregation propensity compared to wild-type and other PD-related mutants A30P, E46K, and G51D [24]. Of note, aggregation of A53T even proceeds in the presence of CtsB and CtsL (Fig. S1 and S2). Moreover, A53T fibrils are more resistant to CtsL when compared to wild-type fibrils (Fig. S3). A LB-derived truncation, Ac1–122, also has enhanced capability to rapidly form fibrils and propagate amyloid formation of the full length protein [12].

Preformed AcA53T and Ac1–122 fibrils (30 μM) were incubated with varying CtsK concentrations (150, 75, and 20 nM) for 16 h at 37 °C and analyzed by LC-MS (Fig. S4). Measured masses and peptide assignments are shown in Tables S8 and S9. Using the lowest

concentration of CtsK, AcA53T and Ac1–122 fibrils showed N- and C-terminal truncations. A very low abundance of smaller peptides derived from the fibril core was also observed (Fig. S4, red traces). These N- and C-terminal cleavage sites are reminiscent to early events seen for Ac-α-syn fibril degradation, including S9/K10, A17/A18, Q109/E110, E114/D115, and S129/E130 (for A53T only). Upon higher CtsK treatments (Fig. S4, blue and magenta traces), the smallest amyloid core fragment generated was 28–109 along with many other smaller peptides derived from similar cleavage sites of the full length wild-type fibrils (Tables S8 and S9).

4.0. Discussion

To visualize these CtsK degradation events at the residue level, we gleaned information from α-syn fibril structures [10, 25-29] solved by cryoelectron microscopy. These contain polymorphic structures, where residues ~36 to 98 can adopt different folds. However, three of the six full-length structures from recombinant proteins look highly similar, perhaps representing the main fibril polymorph containing the bent β-arch kernel [27], which is the structure that we refer to when discussing how CtsK digests α-syn fibrils.

From the structure, there is no density in the N- (residues 1 to 36) and C-terminal (residues 98 to 140) regions, correlating strongly with the proteolytic vulnerability at these sites (Fig. 4). Specifically, initial proteolytic attack by CtsK always occurs in the flexible N- and C-terminus at residues S9/K10, A17/A18, Q109/E110, E114/D115, and S129/E130 (Fig. 4A). This degradation pattern is also reflected in AcA53T and Ac1–122 (except S129/E130), inferring common fibril structural features.

The next sequence of events in digestion are critical into why CtsK is a potent fibril degrading protease. Residues A27 and E28 are not observed in the fibril structure (Fig. 4B), yet they constitute a pivotal cleavage site in destabilizing the fibril core of Ac1–140, AcA53T, and Ac1–122. We hypothesize that upon opening this region, CtsK can then have access to a multitude of cleavage sites shown in Fig. 4. This is reflected from the LC-MS data where upon cleavage at A27/E28, a protease-resistant core corresponding to 28–109 is formed, which is then rapidly attacked at positions L38/Y39, A53/T54, G67/G68, T75/A76, A89/A90, A91/T92, and K96/K97. Many of these peptides; 28–38, 54–67, 68–75, 76–89, 90–96, 92–96 and 97–109 (Fig. 3B) span the entire fibril core, highlighting the potency of CtsK.

Dissecting which of these fibril core degradation events happen first remains ill-defined under the conditions tested. However, based this structure, we speculate that either distal positions L38/Y39 and K96/K97 could be next. With the removal of residues 97–109, it would then permit CtsK easier access to G67/G68, which is part of the β-turn in the kernel and if severed, the fold would destabilize. Interestingly, this cleavage site is also shared with CtsL [19]; but, positions A89/A90 and A91/T92 are unique to CtsK, suggesting that they play a role in facilitating fibril degradation.

Further disaggregation involves additional cuts at A53/T54 and T75/A76. Since residues T75 and A76 reside in the region long implicated in α-syn aggregation propensity and

toxicity [30], once severed, fibril integrity would be compromised. Cutting at the other cleavage site between A53 and T54 presumably would disrupt the steric zipper interface between the two protofibrils (Fig. 4). Importantly, only after these events does further degradation by CtsK occur, generating the smaller peptides observed in Fig. 3A. Interestingly, while we initially expected that AcA53T to have a different degradation profile because of the substitution of the larger Thr sidechain would perturb the interface [10], analogous behavior was observed, suggesting that this point mutation has little impact on structure, which was recently validated [31].

Collectively, our data offer a glimpse into the role both termini play in shielding the core from proteolytic digestion. This is the first such evidence of a protective function of the N- and C-termini, which is not available from the currently published structures due to the flexibility and disordered nature of these regions [10]. Once removed, the protease can gain access to the amyloid core, where CtsK severs a critical β-turn (*e.g.* G67/G68) and destabilizes the protofibril interface (*e.g.* A53/T54). At least thirteen cleavage sites identified from CtsK act on the amyloid core, generating small peptides, destroying the integrity of fibrillar material.

In summary, we have demonstrated that CtsK is a potent protease that can disaggregate wild-type α-syn amyloid fibrils as well as a PD-related mutant (A53T) and C-terminally truncated variant (1–122) found in LBs. While CtsK shares some substrate specificity with CtsL on degrading α-syn fibrils, its efficiency is reflected in its ability to rapidly devour the amyloid core by generating many small peptides from a multitude of cleavage sites. From a lysosomal perspective, there is an increased interest in therapeutically targeting lysosome-dependent pathways that are associated with various diseases [11, 32, 33]. Two promising approaches currently used for targeting lysosomal storage diseases are small molecule and gene therapies [34]. Since CtsK is primarily expressed in osteoclasts, introducing gene expression of CtsK in the brain would offer a new alternative strategy to ameliorate α-syn pathology. Specifically, we envision CtsK degrading fibrils in the lysosome to generate these smaller peptides, that are then further degraded by other cathepsin exopeptidases [15]. Finally, CtsK should be tested against other disease-associated amyloids in future investigations. While premature, it is an exciting prospect to determine whether CtsK or another protease can serve the function of a universal amyloid-degrading ‘amyloidase’.

Supplementary Material

Refer to Web version on PubMed Central for supplementary material.

Acknowledgment

This work is supported by the Intramural Research Program at NHLBI, NIH. Parts of this research were performed on instruments maintained by the NHLBI Biochemistry (LC-MS) and Electron Microscopy (TEM) core. We thank Michael Goedert (MRC Laboratory of Molecular Biology) and Dan Mulvihill (University of Kent) for the pRK172 and pNatB plasmid, respectively. The content of this work is solely the responsibility of the authors and does not necessarily represent the official’s views of the National Institutes of Health.

ABBREVIATIONS

PD	Parkinson’s disease
LBs	Lewy bodies
α-syn	α-synuclein
Cts	cathepsin
ThT	thioflavin-T
Ac	acetylated

REFERENCES

[1]. Spillantini MG, et al., α-Synuclein in filamentous inclusions of Lewy bodies from Parkinson's disease and dementia with Lewy bodies, Proc. Natl. Acad. Sci. U. S. A, 95 (1998) 6469–6473. [PubMed: 9600990]

[2]. Serpell LC, et al., Fiber diffraction of synthetic α-synuclein filaments shows amyloid-like cross-beta conformation, Proc. Natl. Acad. Sci. U. S. A, 97 (2000) 4897–4902. [PubMed: 10781096]

[3]. Schmid AW, et al., α-Synuclein post-translational modifications as potential biomarkers for Parkinson disease and other synucleinopathies, Mol. Cell. Proteomics, 12 (2013) 3543–3558. [PubMed: 23966418]

[4]. van der Wateren IM, et al., C-terminal truncation of α-synuclein promotes amyloid fibril amplification at physiological pH, Chem. Sci, 9 (2018) 5506–5516. [PubMed: 30061982]

[5]. Bassil F, et al., Reducing C-terminal truncation mitigates synucleinopathy and neurodegeneration in a transgenic model of multiple system atrophy, Proc. Natl. Acad. Sci. U. S. A, 113 (2016) 9593–9598. [PubMed: 27482103]

[6]. Games D, et al., Reducing C-Terminal-truncated α-synuclein by immunotherapy attenuates neurodegeneration and propagation in Parkinson's disease-like models, J. Neurosci, 34 (2014) 9441–9454. [PubMed: 25009275]

[7]. Sorrentino ZA, et al., Carboxy-terminal truncations of mouse α-synuclein alter aggregation and prion-like seeding, FEBS Lett., 594 (2020) 1271–1283. [PubMed: 31912891]

[8]. Sorrentino ZA, et al., Physiological C-terminal truncation of α-synuclein potentiates the prion-like formation of pathological inclusions, J. Biol. Chem, 293 (2018) 18914–18932. [PubMed: 30327435]

[9]. Terada M, et al., The effect of truncation on prion-like properties of α-synuclein, J. Biol. Chem, 293 (2018) 13910–13920. [PubMed: 30030380]

[10]. Ni X, et al., Structural insights into α-synuclein fibril polymorphism: Effects of Parkinson's disease-related c-terminal truncations, J. Mol. Biol, 431 (2019) 3913–3919. [PubMed: 31295458]

[11]. Wallings RL, et al., Lysosomal dysfunction at the centre of Parkinson's disease and frontotemporal dementia/amyotrophic lateral sclerosis, Trends Neurosci, 42 (2019) 899–912. [PubMed: 31704179]

[12]. McGlinchey RP, et al., C-terminal α-synuclein truncations are linked to cysteine cathepsin activity in Parkinson's disease, J. Biol. Chem, 294 (2019) 9973–9984. [PubMed: 31092553]

[13]. Webb JL, et al., α-Synuclein is degraded by both autophagy and the proteasome, J. Biol. Chem, 278 (2003) 25009–25013. [PubMed: 12719433]

[14]. Kaushik S, Cuervo AM, The coming of age of chaperone-mediated autophagy, Nat. Rev. Mol. Cell Biol, 19 (2018) 365–381. [PubMed: 29626215]

[15]. Turk V, et al., Cysteine cathepsins: From structure, function and regulation to new frontiers, BBA-Proteins Proteomics, 1824 (2012) 68–88. [PubMed: 22024571]

[16]. Kramer L, et al., The future of cysteine cathepsins in disease management, Trends Pharmacol. Sci, 38 (2017) 873–898. [PubMed: 28668224]

[17]. Vidak E, et al., Cysteine cathepsins and their extracellular roles: Shaping the microenvironment, Cells, 8 (2019) 24.

[18]. McGlinchey RP, Lee JC, Cysteine cathepsins are essential in lysosomal degradation of α-synuclein, Proc. Natl. Acad. Sci. U. S. A, 112 (2015) 9322–9327. [PubMed: 26170293]

[19]. McGlinchey RP, et al., Taking a bite out of amyloid: mechanistic insights into α-synuclein degradation by cathepsin L, Biochemistry, 56 (2017) 3881–3884. [PubMed: 28614652]

[20]. Jakes R, et al., Identification of two distinct synucleins from human brain, FEBS Lett, 345 (1994) 27–32. [PubMed: 8194594]

[21]. Johnson M, et al., Targeted amino-terminal acetylation of recombinant proteins in E. coli, PLoS One, 5 (2010) e15801. [PubMed: 21203426]

[22]. Rodriguez JA, et al., Structure of the toxic core of α-synuclein from invisible crystals, Nature, 525 (2015) 486–490. [PubMed: 26352473]

[23]. Anderson JP, et al., Phosphorylation of Ser-129 is the dominant pathological modification of α-synuclein in familial and sporadic Lewy body disease, J. Biol. Chem, 281 (2006) 29739–29752. [PubMed: 16847063]

[24]. Flynn JD, et al., Structural features of α-synuclein amyloid fibrils revealed by Raman spectroscopy, J. Biol. Chem, 293 (2018) 767–776. [PubMed: 29191831]

[25]. Boyer DR, et al., Structures of fibrils formed by α-synuclein hereditary disease mutant H50Q reveal new polymorphs, Nat. Struct. Mol. Biol, 26 (2019) 1044–1052. [PubMed: 31695184]

[26]. Fitzpatrick AWP, Saibil HR, Cryo-EM of amyloid fibrils and cellular aggregates, Curr. Opin. Struct. Biol, 58 (2019) 34–42. [PubMed: 31200186]

[27]. Li BS, et al., Cryo-EM of full-length α-synuclein reveals fibril polymorphs with a common structural kernel, Nat. Commun, 9 (2018) 10. [PubMed: 29295980]

[28]. Li YW, et al., Amyloid fibril structure of α-synuclein determined by cryoelectron microscopy, Cell Res, 28 (2018) 897–903. [PubMed: 30065316]

[29]. Guerrero-Ferreira R, et al., Cryo-EM structure of α-synuclein fibrils, eLife, 7 (2018) 18.

[30]. Giasson BI, et al., A hydrophobic stretch of 12 amino acid residues in the middle of α-synuclein is essential for filament assembly, J. Biol. Chem, 276 (2001) 2380–2386. [PubMed: 11060312]

[31]. Sun YP, et al., Cryo-EM structure of full-length α-synuclein amyloid fibril with Parkinson's disease familial A53T mutation, Cell Res., 30 (2020) 360–362. [PubMed: 32203130]

[32]. Platt FM, Emptying the stores: lysosomal diseases and therapeutic strategies, Nat. Rev. Drug Discov, 17 (2018) 133–150. [PubMed: 29147032]

[33]. Stoka V, et al., Lysosomal cathepsins and their regulation in aging and neurodegeneration, Ageing Res. Rev, 32 (2016) 22–37. [PubMed: 27125852]

[34]. Marques ARA, Saftig P, Lysosomal storage disorders - challenges, concepts and avenues for therapy: beyond rare diseases, J. Cell Sci, 132 (2019) 14.

Highlights

- Cathepsin K was identified as a potent disaggregase of α-syn fibrils
- Mechanistic insights were revealed by detailed peptide mapping by LC-MS
- N- and C-termini protect the amyloid core from proteolytic attack
- Critical cleavages sites involved in degradation were identified
- Cathepsin K offers therapeutic approach for decreasing fibril load in PD

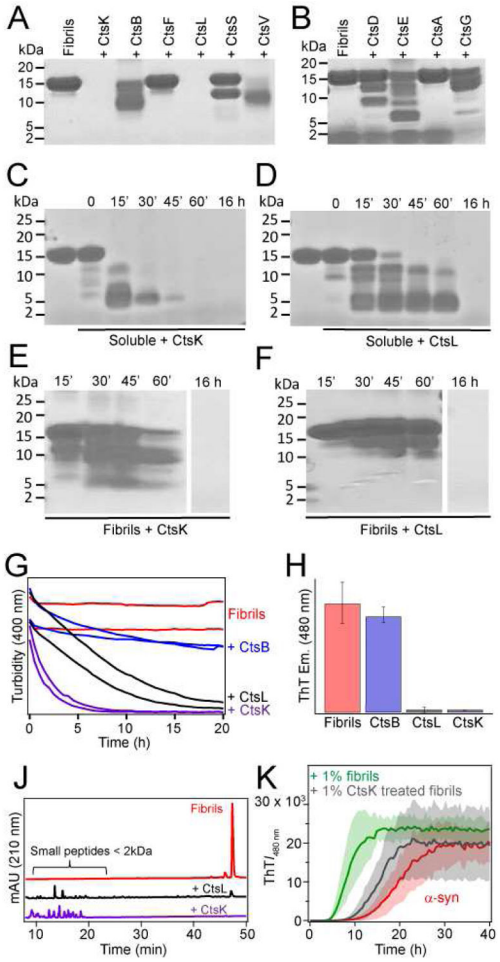

Fig. 1. Screening for a potent disaggregase of α-syn fibrils.

(A) and (B) SDS-PAGE analysis of preformed fibrils (60 μM) incubated with cathepsins (150 nM in 50 mM NaOAc, 20 mM NaCl, 5 mM DTT, pH 5) for 16 h at 37 °C. SDS-PAGE analysis of soluble (C and D) and fibrillar (E and F) α-syn incubated with either CtsK or CtsL (15–150 nM in 50 mM NaOAc, 20 mM NaCl, 5 mM DTT, pH 5) as a function of time at 37 °C. (G) Disaggregation kinetics of α-syn fibrils (35 μM) incubated in the absence (red) and presence of CtsB (blue), CtsL (black) and CtsK (purple) at pH 5 ([Cts] = 150 nM, pH 5 at 37 °C) monitored by turbidity. ThT fluorescence (H) and LC (J) measured at the end of the reactions shown in panel G. MS analysis for CtsK treatment is shown in Table S1. (K) Seeding reactions of soluble α-syn (50 μM) at pH 7.4 in the absence (red) and presence of either 1 % fibrils (green) or CtsK-treated fibrils (gray) monitored by ThT fluorescence at 37 °C. Solid lines and shaded areas represent averages and standard deviations ($n \geq 5$).

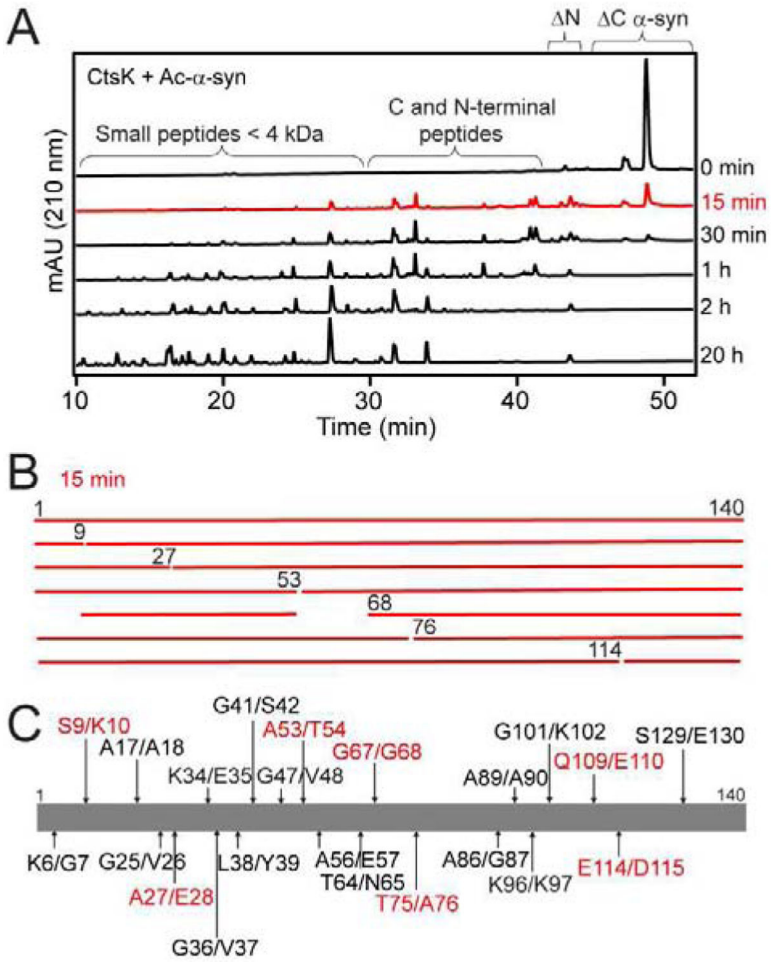

Fig. 2. CtsK degradation of soluble Ac-α-syn at pH 5.

(A) LC traces taken as a function of time of soluble Ac-α-syn (15 μM) incubated with CtsK (5 nM) at pH 5 and monitored at 210 nm. Peptide fragments are depicted as either N- or C-terminally-derived from soluble Ac-α-syn as shown. (B) Peptide fragments generated after 15 min incubation with CtsK. (C) Peptide mapping of all observable CtsK cleavage sites of Ac-α-syn at 15 min (red) and 30 min to 2 h (black). MS data are shown in Tables S2 and S3.

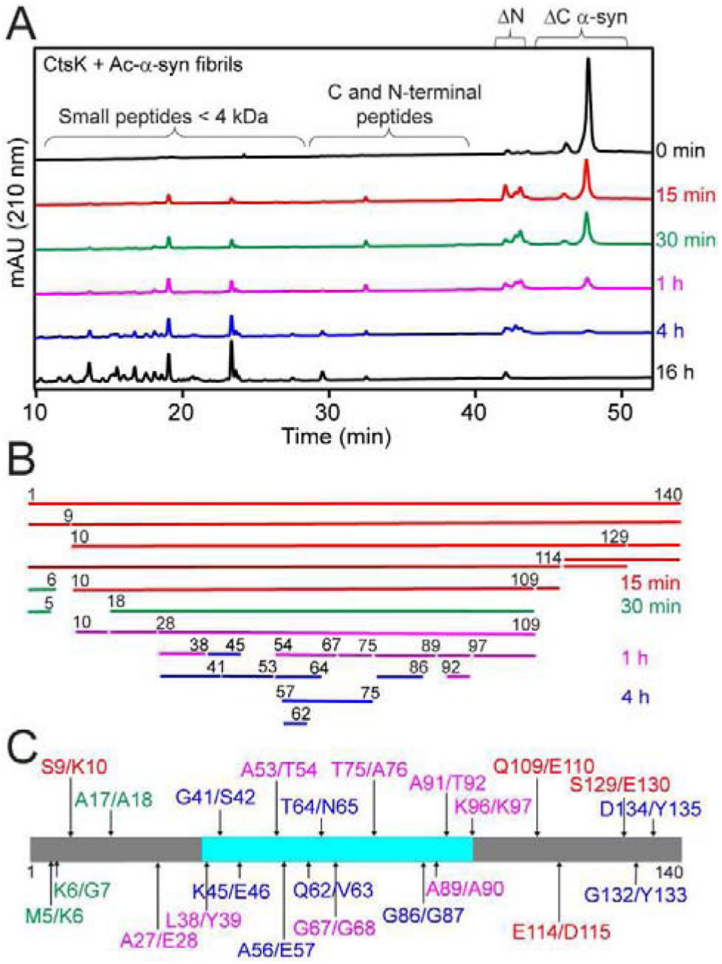

Fig. 3. Fibril degradation by CtsK.

(A) LC traces taken as a function of time of preformed fibrils (15 μM) incubated with CtsK (20 nM) at pH 5 for 16 h at 37 °C. (B) Peptide fragments generated after 15 min (red), 30 min (green), 1 h (magenta) and 4 h (blue) incubation with CtsK (20 nM). (C) Peptide mapping of all observable CtsK cleavage sites of fibrils at times 15 min to 4 h colored as in A. Cryo-EM amyloid core (residues 36–96) is indicated in cyan [10]. MS data are shown in Table S5 and S6.

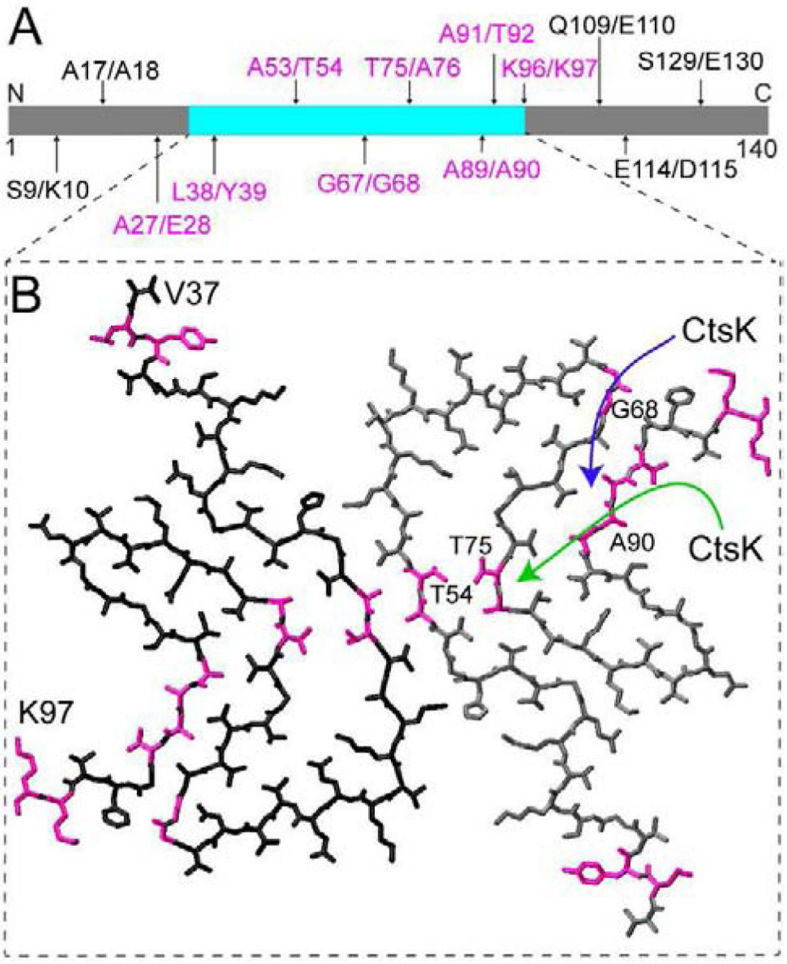

Fig. 4. CtsK activity mapped onto cryo-EM fibril structure.

(A) Schematic representation of the primary amino acid sequence of Ac-α-syn highlighting CtsK activity on fibrils after 15 min (black) and 1 h (magenta). Cryo-EM amyloid core (residues 37–97) is shown in cyan. (B) Critical cleavage sites for disassembling the amyloid core (PDB code 6OSJ [10]) are colored magenta. Two putative directions of CtsK attack are shown by arrows.